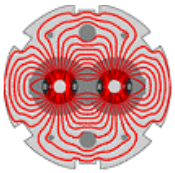

LHC Project Note 191

1999-06-03

(maciej.chorowski@cern.ch)

Thermo - hydraulic analysis of a cryogenic jet: application to helium recovery following resistive transitions in the LHC

M. Chorowski, P. Grzegory, G. Konopka

Wroclaw University of Technology
Institute of Power Engineering and Fluid Mechanics

Summary

A resistive transition (quench) of the LHC sector magnets will be followed by cold helium venting to a quench buffer volume of 2000 m^3 at ambient temperature. The volume will be composed of eight medium-pressure (2 MPa) gas storage tanks made of carbon steel, which constrains the temperature of the wall to be higher than -50 ^oC (223 K). Possible spot cooling intensity and thermo-mechanical stresses in the tank wall following helium injection have been analysed previously and the aim of the present study is experimental verification of basic assumptions concerning cryogenic jet parameters and heat transfer between jet crown and tank wall. For this purpose jet diameter, velocity profile and convective heat transfer between jet and steel plate have been measured. A simple jet model description based on momentum conservation has been proposed. Then, the lowest possible temperature of the tank wall which may occur has been assessed.

1. Introduction

A resistive transition (quench) of the LHC magnets will be followed by helium discharge from magnet cold mass to helium recovery system composed of vacuum-insulated header D in cryogenic distribution line QRL, medium pressure tanks and auxiliaries [1]. Then about 1400 kg of helium per sector will have to be vented to a quench buffer volume of 2000 m^3 at ambient temperature. The volume will be composed of eight medium-pressure gas storage tanks, 250 m^3 each. The medium-pressure tanks are made of carbon steel, which constrains the temperature of the wall to be higher than -50 ^oC (223 K). The temperature of the helium flowing into a single tank will be of about 12 K and its mass flow of about 2.5 kg/s for about 70 seconds. To avoid a single jet formation, pressurised helium will be injected through a number of small orifices drilled in a dedicated distributor pipe inside the tank.

A possible spot cooling intensity as well as thermo-mechanical stresses in the tank wall following helium injection have been analysed [2, 3]. The spot cooling intensity analysis has been based on the assumption of linear growth of the jet crown diameter along the jet axis. The uniform velocity profile has been calculated on the assumption of the axial momentum flux being constant over the area of the jet crown. Heat transfer coefficient has been calculated from the following dimensionless Eq. (1).

$$Nu = 0{,}57 \cdot Re^{0,5} \cdot Pr^{0,3} \tag{1}$$

It has been calculated [2] that cold helium injection through a number of orifices in a dedicated pipe will not provoke a state of strains and stresses in the tank wall exceeding the admissible values obtained according to CODAP 90. The temperature of the cold spot will decrease to about 226 K and will stay within the carbon steel operation limit i.e. above –50 ^oC.

It has been also recommended to verify experimentally the assessment of the jet crown area, the hypothesis of turbulent mixing of helium in the crown, the velocity profile and the heat fluxes to the tank wall.

1.1 Aim of the study

The aim of the present analysis is a predictive model description and experimental verification of turbulent cryogenic jet parameters such as:

- jet crown area – assumption of linear growth of the jet diameter,
- mean velocity profile along the jet axis,
- convective heat transfer between jet and solid object (e.g. tank wall).

2. Test facilities

The vented gases were nitrogen and helium. Nitrogen was supplied from a 150 dm^3 dewar vessel of maximum pressure 2 MPa, while helium was vented from a 11000 gallon container of inside pressure equal to 0.33 MPa.

Fig.1 shows the conceptual scheme of a test rig used during the experiment. The vent was designed in such way to make possible changes in the orifice diameter (1, 3 and 5 mm) and it was supplied with nitrogen or helium through a transfer line connected to LN_2 or LHe container. Due to the gas pressures inside the nitrogen vessel (above 1 MPa) and helium container (0.33 MPa) the velocity at the outlet was equal to the speed of sound for both nitrogen and helium. Nitrogen was vented into the air at a temperature of 290 K and helium was vented into the air at a temperature of 275 K.
The jet temperature was measured by type T thermocouples (copper versus Constantan) placed on the thin wire along the jet axis at different distances from the vent.
Velocity was measured by means of a vane anemometer also at different distances.
The jet diameter was measured by means of a simple device. It was a rod with light flaps located every 2.5 cm. A flowing jet caused the flaps to move enabling an estimation of the jet diameter.

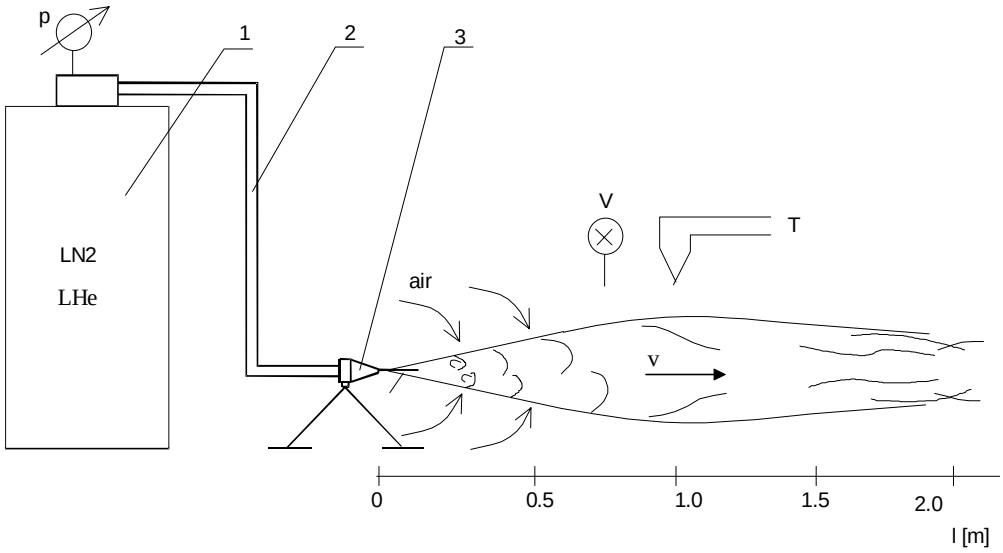

Fig.1. Test rig, 1 – LN2 / LHe vessel, 2 – transfer line, 3 – orifice, p – pressure gauge, v – velocity meter (vane anemometer), T – temperature sensor (thermocouple)

3. Experimental results

3.1. Diameter of the jet

During venting of nitrogen and helium, the jet diameter along the axis was measured. The summary results are shown in Fig. 2. The measurements have confirmed an assumption that the cone angle does not depend on the orifice diameter or the gas vented. It is constant and of about 13 degrees. It means that the diameter of the jet crown changes linearly along the jet axis. The result remains in good agreement with the data used in [2, 3] for jet crown diameter assessment, where the cone angle calculated was 12.6 degrees.

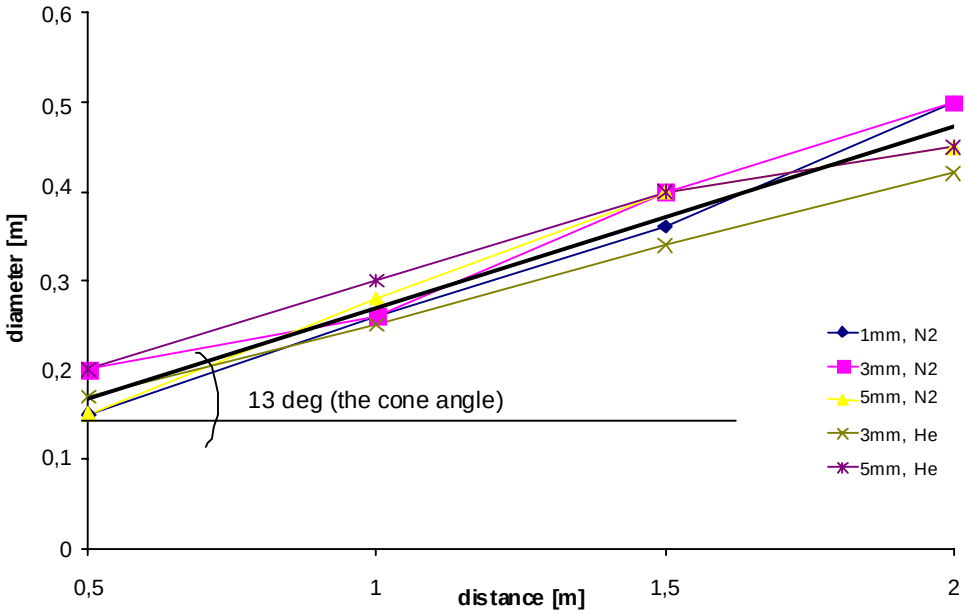

Fig. 2. Jet diameter measured along the axis

3.2 Temperature profile along the jet axis

For vented nitrogen and helium, the temperature along the jet axis was measured. The results are shown in Fig. 3.

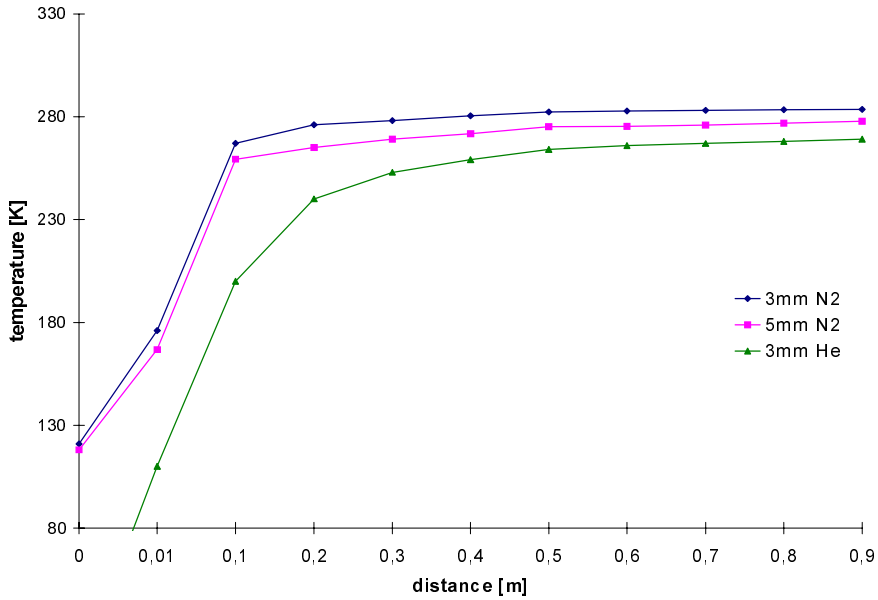

Fig. 3. Centreline temperature profile measured along the jet axis

The orifice diameter was 3 mm and 5 mm for nitrogen, and 3 mm for helium. The ambient temperature was 291 K for nitrogen and 275 K for helium. The results show that the biggest intake of air occurs in the first region of the jet. During the first 20 cm the jet temperature rises approximately by 160 K for nitrogen and 180 K for helium. Then along the next 1.5 m it rises only by about 15 K and 40 K respectively. We assume that the temperature increase results from the mixing process only.

The temperature shown in Fig.3 is the lowest temperature measured in the centre of the jet.
Fig. 4 shows the temperature distribution across the nitrogen jet crown measured at the distance of 0.4 m from the 3 mm orifice. The difference between the jet centreline and ambient temperature is of about 13 K.

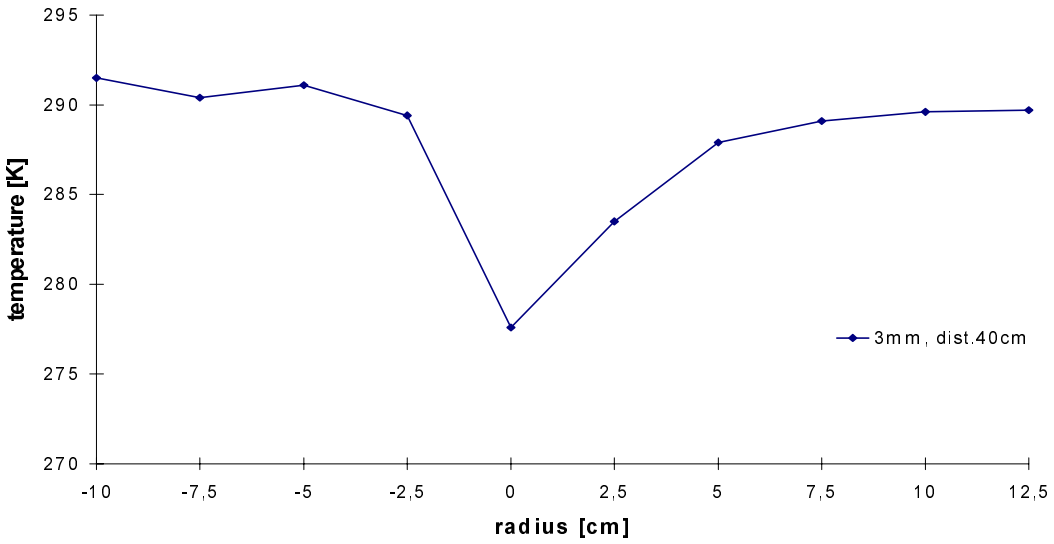

Fig. 4. Temperature profile across nitrogen jet crown (measured)

3.3. Velocity profile along the jet axis

3.3.1. Nitrogen

The jet velocity was measured for different orifice diameters (1, 3 and 5 mm). The results are shown in Fig.5. At the vent the velocity was of 183 m/s i.e. the speed of sound for 10 bar pressure and corresponding saturation temperature.
The jet velocity decreases along the jet axis. Such a velocity profile results from conservation of momentum- Eq. (2), along the jet axis.

$$\frac{d(\rho \cdot v^2 \cdot A)}{dx} = 0 \tag{2}$$

It follows from Eq. (2) that for outlet cross section (subscript 1) and a cross section at a distance x from the vent:

$$\rho_1 \cdot v_1^2 \cdot A_1 = \rho(x) \cdot v(x)^2 \cdot A(x) \tag{3}$$

Taking into consideration constant parameters at the outlet of the orifice, the relation defining velocity variation along the jet axis- $v(x)$ is as follows– Eq.(4).

$$v(x) = \sqrt{\frac{\rho_1 \cdot v_1^2 \cdot A_1}{\rho(x) \cdot A(x)}} \tag{4}$$

where: ρ_1 - nitrogen density at the orifice outlet; v_1- nitrogen velocity at the orifice outlet , A_1- orifice outlet cross section area, x – distance from the vent, $\rho(x)$ -nitrogen density along jet axis (for p = 0.1 MPa), $A(x)$ – jet cross section area dependent on distance from the orifice outlet:

$$A(x) = \frac{\pi \cdot (D(x))^2}{4} \tag{5}$$

where: $D(x)$ is the jet diameter and

$$D(x) = 0.23 \cdot x \tag{6}$$

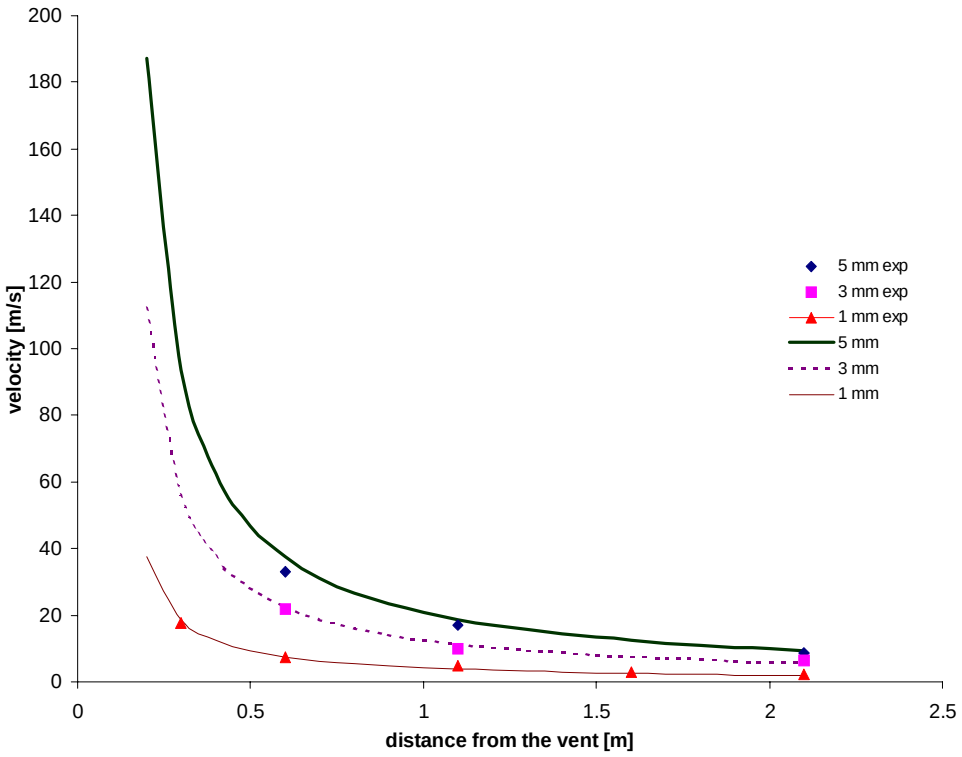

Fig. 5. Centreline velocity along the jet axis (measured - dots and calculated - lines)

The number 0,23 results from the fact that jet cone angle is constant and equals 13 degrees- see Fig. 2. The experimental velocity profile is compared with that calculated from Eq. (4) and is shown in Fig. 5. The calculations were accomplished for the distance x > 0.20 m where the jet temperature and pressure could also be assumed constant (see Fig. 3). As a consequence the jet density could be considered as constant. Considering the good fit between experimental and calculated data such an assumption gives enough accuracy for engineering applications.

As verification of our model a warm nitrogen jet (i.e. at ambient temperature) was experimented for different outlet pressures. The results are shown in Fig.6.

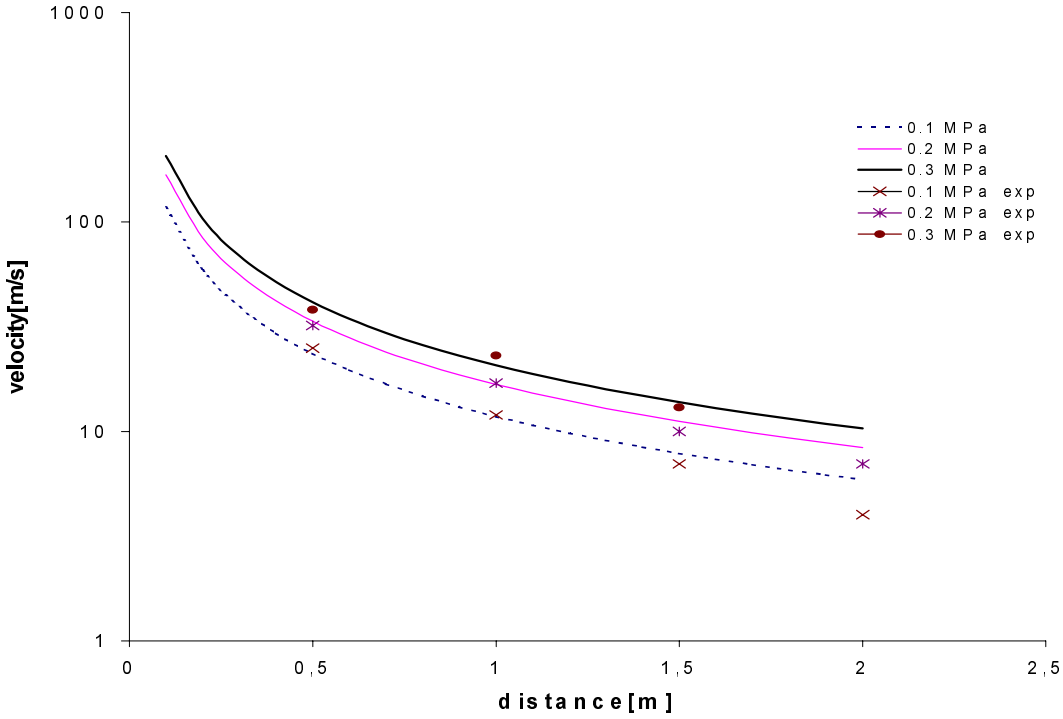

Fig. 6. Velocity distribution for warm jet at different outlet pressures (measured - dots, calculated - lines)

3.3.2 Helium

The velocity profile for a helium jet vented into air results from Eq. (4). Due to the difference between helium and air densities, the jet density can not be assumed constant and is given by Eq. (7)

$$\rho(x) = g_{air}(x) \cdot \rho_{air} + g_{He}(x) \cdot \rho_{He} \qquad (7)$$

where: ρ_{He} , ρ_{air} are densities of helium and air for $T = T(x)$ and g_{air} , g_{He} are mass concentrations of air and helium in the jet, x denotes the distance from the vent.

It is assumed that there is a jet zone close to the orifice (for x less than x'- see Fig. 7) where no mixing of helium and air occurs (jet is composed only of helium). For this zone the jet diameter increase results from helium expansion until the jet pressure reaches the ambient pressure. For x less than x' the jet temperature is constant: $T(x)=T_0$.
For x values exceeding the distance x' the mixing process starts and the jet cross section increases due to the uptake of air.

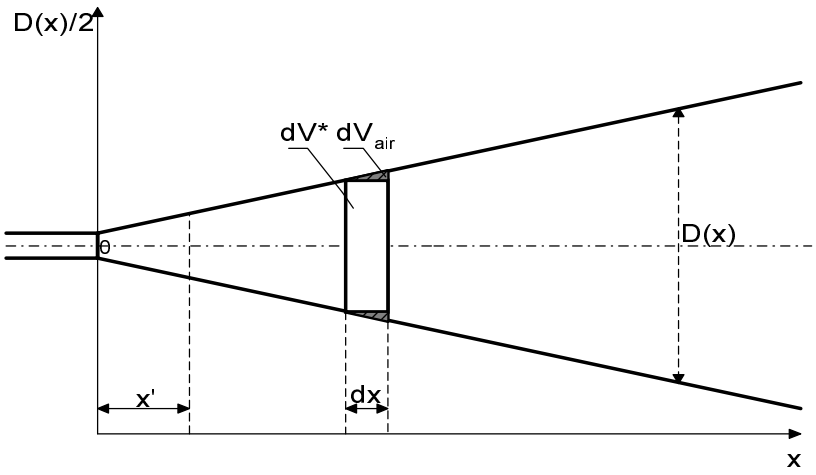

Fig. 7. Schematic representation of a turbulent cryogenic jet

The distance x' can be assessed by solving the set of Eq. (8, 9) combined with Eq. (5, 6):

$$A_1 \cdot \rho_1 \cdot v_1 = A(x') \cdot \rho(x') \cdot v(x') \tag{8}$$

$$A_1 \cdot \rho_1 \cdot v_1^2 = A(x') \cdot \rho(x') \cdot v(x')^2 \tag{9}$$

where: $\rho(x')$ is helium density at the distance x' for ambient pressure and temperature $T = T_0$ and index "1" denotes the jet parameters at the outlet from the orifice.

The average mass concentration of air in the jet at the distance $x+dx$ is given by Eq. (10). This equation results from the conical geometry of the jet – see Fig.7.

$$g_{air}(x+dx) = \frac{dM_{air} + M(x) g_{air}(x)}{M(x+dx)} \tag{10}$$

where: dM_{air} is the mass of the air taken in the distance interval dx, $M(x)$ is the total mass of the jet at the distance x, $M(x+dx)$ is the total mass of the jet at the distance $x+dx$.

$$dM_{air} = \frac{dV_{air}}{dx} dx \cdot \rho_{air} \quad , \tag{11}$$

$$M(x+dx) = \frac{dM_{air}}{dx} dx + M(x) \, , \tag{12}$$

$$\frac{dV_{air}(x)}{dx} = \frac{dV(x)}{dx} - \frac{dV^*(x)}{dx} \tag{13}$$

The calculated and measured velocity distribution along the jet axis is presented in Fig.8.

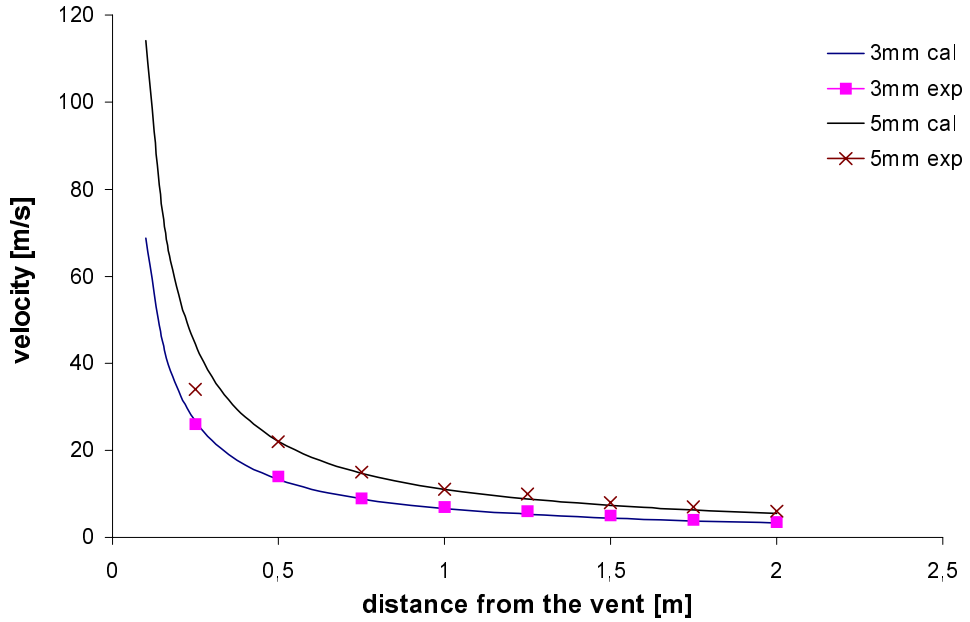

Fig. 8. Velocity distribution along helium jet axis (measured - dots, calculated - lines)

3.4. Heat transfer measurements

The objective of this experiment was the estimation of the heat flux between the cryogenic jet and a carbon steel plate. The conceptual scheme of the test rig is shown in Fig. 9. The diameter of the plate was 0.116 m and its thickness 0.02 m. The mass of the plate was 1.5 kg. The back and edges of the plate were insulated. The temperature of the plate was measured in three points. Because the good thermal diffusivity of carbon steel, temperature differences across the plate cross-section are small and the average value can be taken for further considerations.

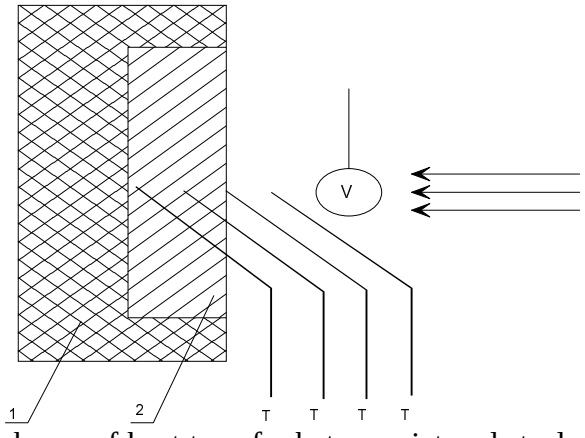

Fig. 9. Conceptual scheme of heat transfer between jet and steel plate experiment, 1 – insulation, 2 – steel plate, T – temperature sensors (thermocouples), V – vane anemometer

The heat flux between the steel plate and the jet was calculated according to the formula:

$$\dot{Q} = M \cdot c_p \cdot \frac{\Delta T}{\Delta t} \tag{14}$$

where M – denotes mass of the plate, ΔT is average temperature drop during the time interval Δt, c_p stands for heat capacity of the steel plate.
A heat transfer coefficient h results from Eq. (14) and is equal to:

$$h = \frac{\dot{Q}}{A \cdot (T_p - T_J) \cdot \Delta t} \tag{15}$$

where: T_p is average steel plate temperature and T_J is jet temperature close to the plate, A stands for heat exchange area.
To describe the process of convective heat transfer between steel plate and jet we propose to use the following formula [4]

$$Nu = c \cdot Re^n \tag{16}$$

$$\mathrm{Re} = \frac{v \cdot \rho \cdot \sqrt{A}}{\eta} \quad , \quad Nu = \frac{h \cdot \sqrt{A}}{\lambda} \tag{16a}$$

where: ρ- jet density, A- jet cross section area, η- jet viscosity, λ- jet conductivity, Nu- Nusselt number, Re- Reynolds number, h- heat transfer coefficient.

In the literature [4] the following coefficients are recommended c = 0.107 and n = 0.7.

3.4.1 Procedure of experimental verification of coefficient *n* in Eq. (16)

Fig. 10 shows a typical measured temperature transient in the steel plate. On that basis the transient heat flux was calculated from Eq. (14) and is shown in Fig. 11. Knowing heat flux and temperature difference between jet and steel plate, the transient values of heat transfer coefficient was calculated from Eq. (15). Finally the average heat transfer coefficient was calculated as a mean of the transient values. In the following it is called experimental – h_{exp}. The heat transfer coefficient is then obtained from Eq. (16) and in the further analysis it is named calculated – h_{calc}. Comparing experimental and calculated heat transfer coefficients (see Fig. 12) factor n in Eq. (16) has been modified in order to fit experimental data. We have found n of 0.77 in a good agreement with measured results.
The above procedure was applied in all cases of heat transfer experiment (for different orifice diameters, different distances from the orifice outlet and different gas- nitrogen or helium). The summary of these experiments is presented in Fig. 13, where ratios of experimental and calculated heat transfer coefficients are shown.
The horizontal axis of Fig. 13 describes the orifice diameter (first number) and steel plate distance from the outlet of the vent (second number). The first six experiments were done with nitrogen at 10 bar pressure and saturation temperature, the last one was done with helium at 3 bar pressure and temperature of 60 K. Standard deviation is 11 %.

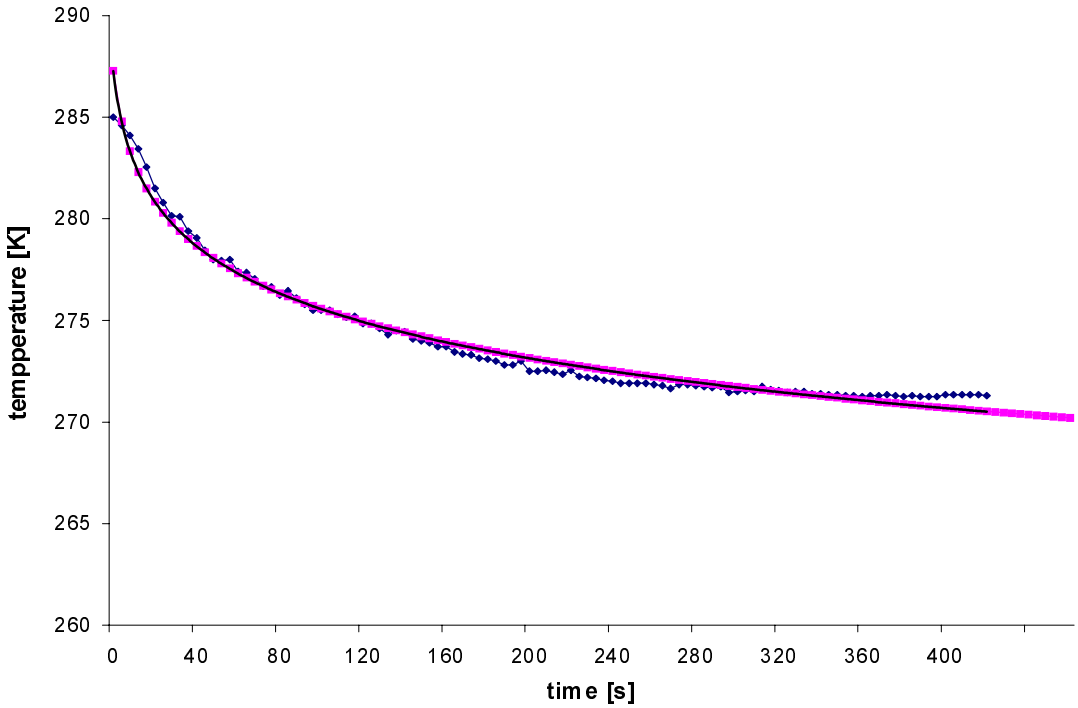

Fig. 10. Transient average temperature of steel plate (measured) and trend line (orifice 3 mm, distance 0,5 m)

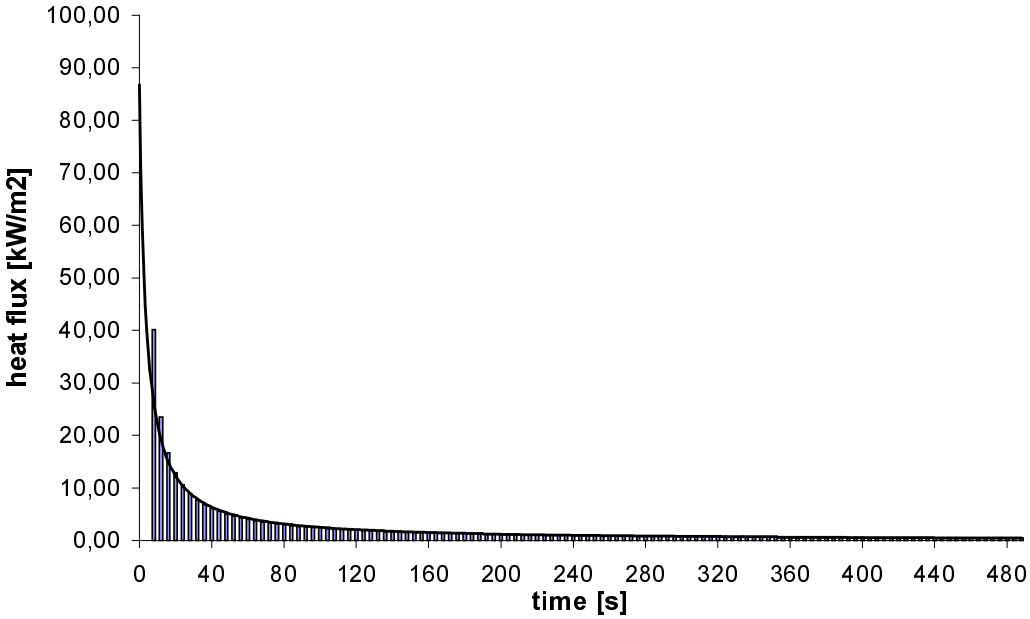

Fig. 11. Transient heat flux from nitrogen jet to a steel plate (calculated for orifice diameter 3 mm and distance 0,5 m)

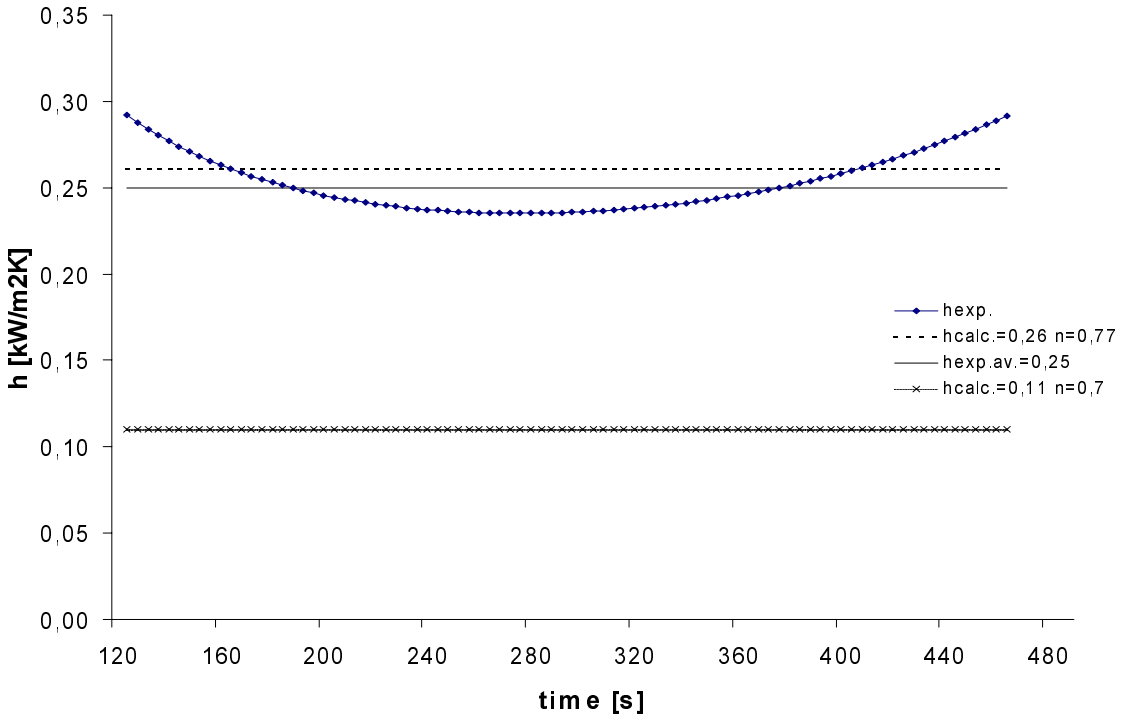

Fig. 12. Transient experimental and calculated heat transfer coefficient (for orifice diameter 3 mm and distance from the vent 0,5 m)

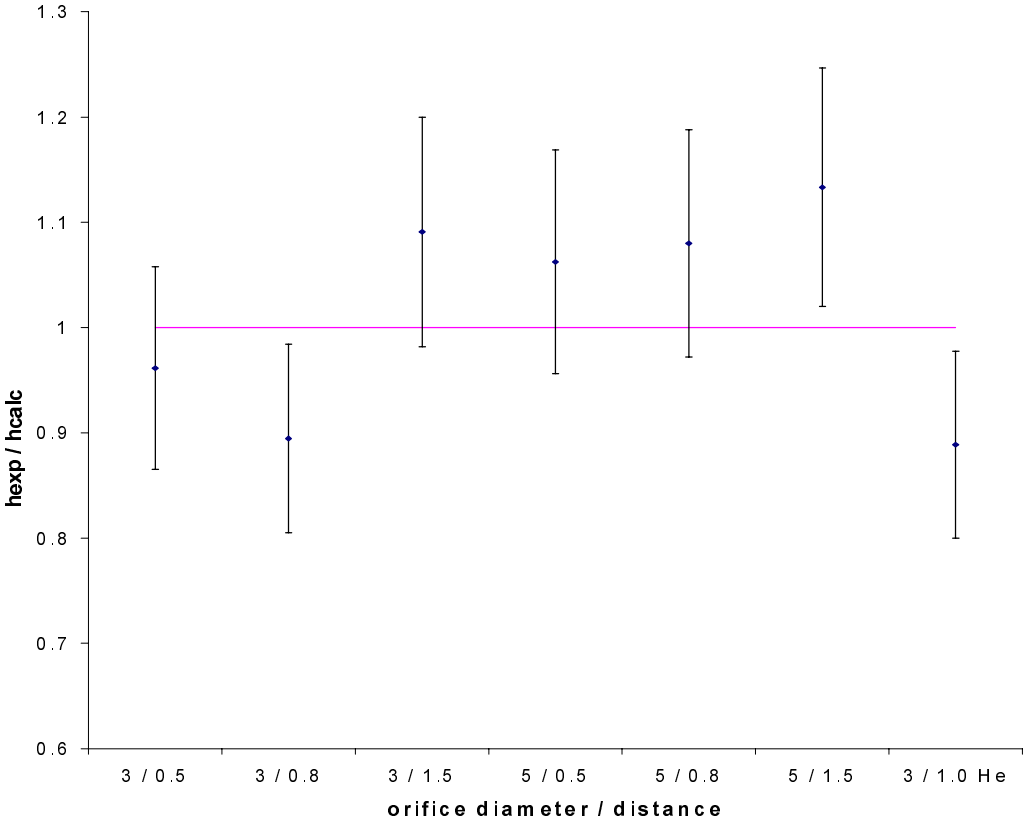

Fig.13. Ratio of experimental and calculated heat transfer coefficient, h_{exp} – average heat transfer coefficient obtained experimentally, h_{calc} – heat transfer coefficient calculated from Eq.(16)

On the basis of Fig. 13 the validity of the Eq.(16) with the coefficients c = 0.107 and n = 0.77 was established. Fig.14 shows the calculated heat transfer coefficient for nitrogen and helium as a function of the distance from the vent. The heat transfer coefficient strongly decreases with increasing distance.

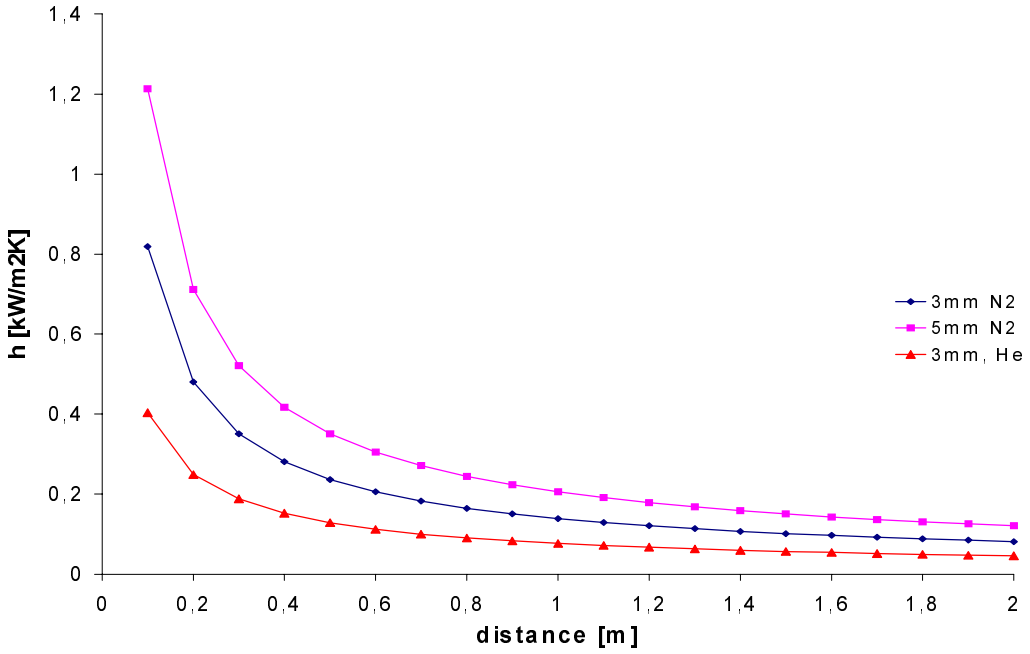

Fig. 14. Calculated (Eq. 16) convective heat transfer coefficient versus distance from the vent (venting to air at the temperature of 290 K), initial conditions were: for nitrogen – pressure 10 bar, saturated temperature, for helium – pressure 0.2 MPa, temperature 60 K

4. Heat exchange between helium and medium-pressure gas storage tank wall

We assume that the helium is injected into a medium-pressure tank through a number of orifices drilled in the pipe threading its way along the tank axis (see Fig. 15). The diameter of each orifices is 5 mm. The temperature of the injected helium is 15 K and its density 60 kg/m3, the helium being injected with the speed of sound.

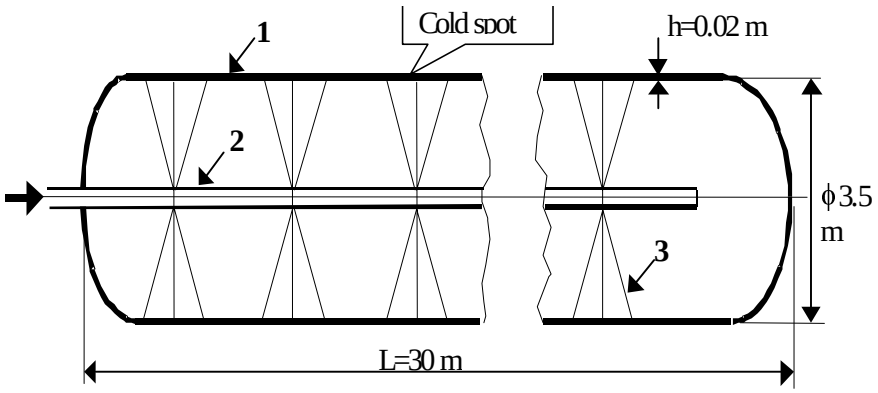

Fig. 15. Helium storage tank with the axisymmetric conical jets: 1- medium-pressure tank, 2- inner tube with drilled orifices, 3- jet

Fig.16 shows the evolution of average helium temperature and pressure in the medium-pressure gas storage tanks following resistive transition of an LHC sector [1]. At a distance of 1.75 m from the orifice, the jet temperature can be treated as equal to the average helium temperature in the tank.

For these conditions the heat transfer between the tank wall and the helium jet crown was calculated from Eq. 16. The heat transfer coefficient is a function of pressure and temperature and as both are functions of time the heat transfer coefficient changes with respect to time, as well. It is shown in Fig. 17.

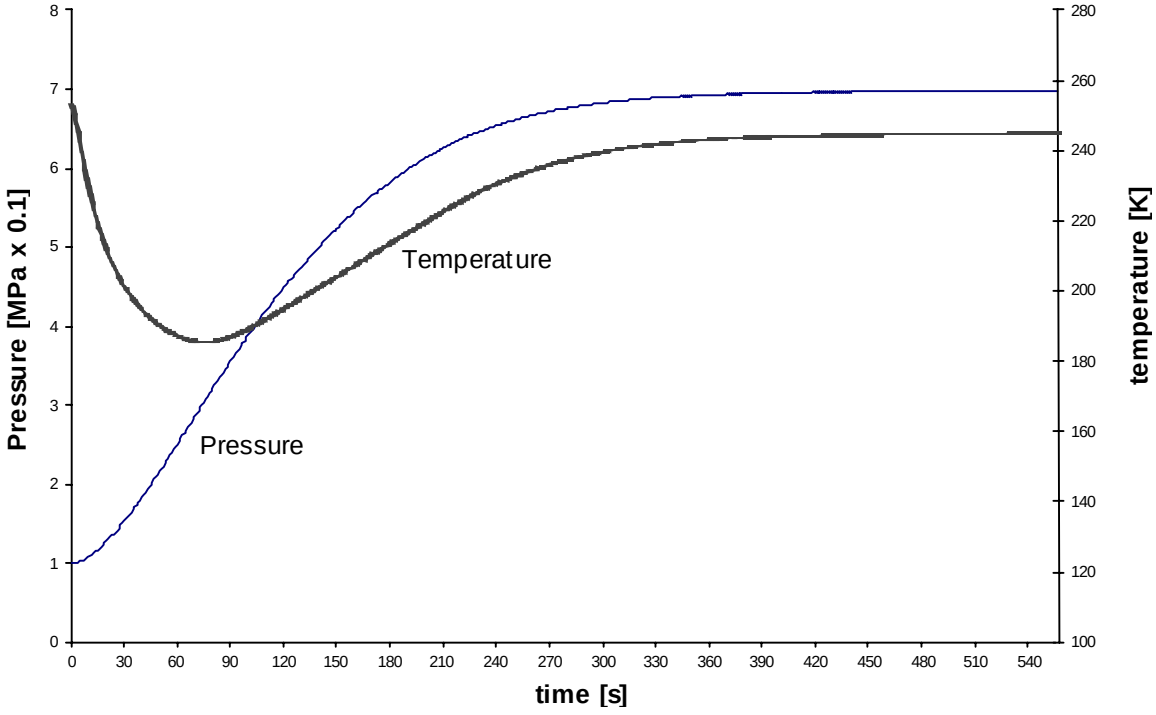

Fig. 16. Calculated [1] helium temperature and pressure in a medium-pressure tank during discharge of line D following a LHC sector quench, initial temperature and pressure 253 K and 0.1 MPa respectively

Then the lowest temperature (cold spot – see Fig. 15) of the tank wall has been calculated. The conservative approach was applied and no conductive heat transfer from a cold spot to other parts of the tank wall as well as convective heat transfer to the environment was taken into account (adiabatic conditions of a cold spot cooling). The calculated cold spot temperature evolution is shown in Fig. 18.

The temperature of the cold spot lowers by 47 K from its initial value. Provided initial tank wall temperature is not less than 270 K, the lowest temperature of the cold spot will not exceed the minimum admissible temperature of 223 K (-50^{o}C) for the carbon steel grade P355NL2.

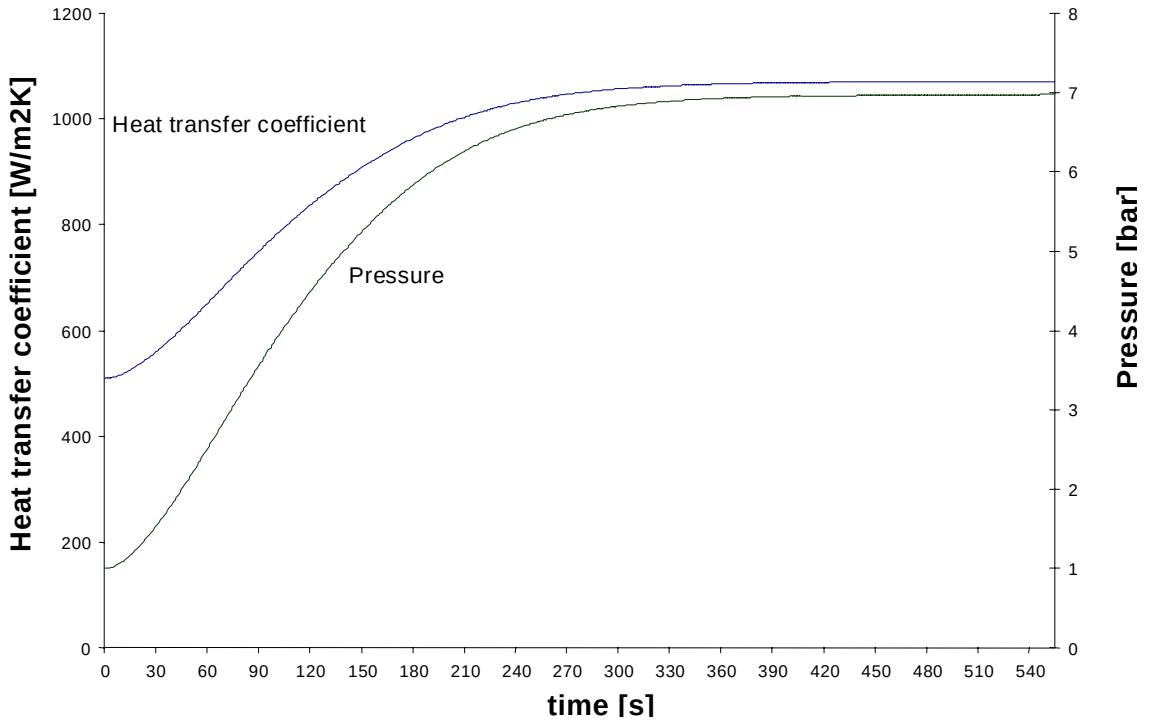

Fig. 17. Heat transfer coefficient and pressure evolution with respect to time during discharge of line D, following a LHC sector quench

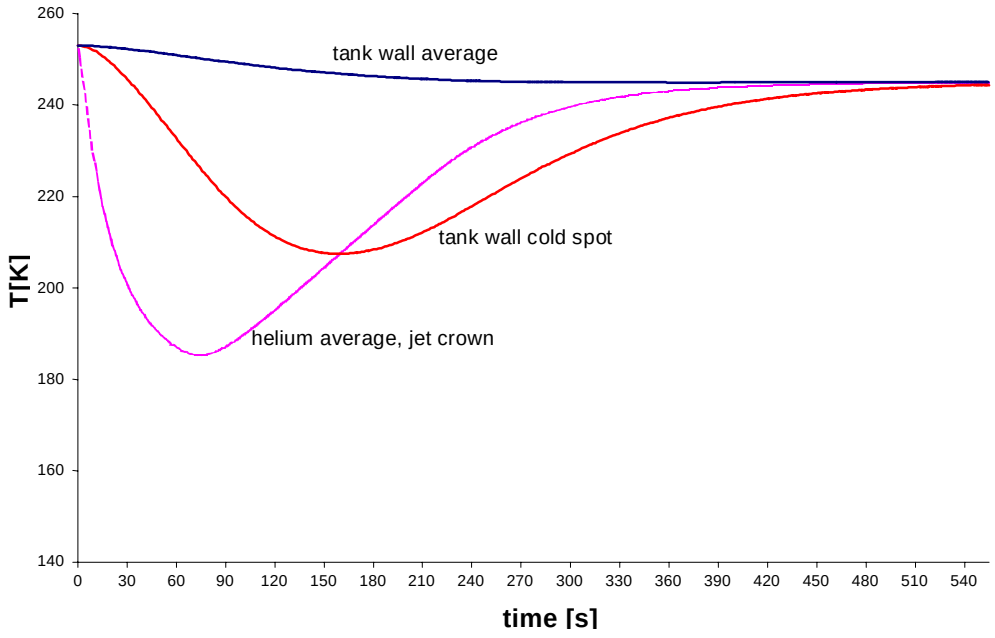

Fig. 18. Average and cold spot temperature evolution of the tank wall

5. Conclusions

Thermal and hydraulic assumptions of the theoretical analysis [2] concerning thermo-mechanical consequences of a cold helium injection following resistive transition of LHC magnets, into medium-pressure gas storage tanks made of carbon steel, has been validated. The tanks may serve as efficient quench buffer vessels, provided that the cold helium injection is distributed over a sufficient length to form a number of jets.

The temperature of the cold spots will decrease by about 47 K.

A turbulent cryogenic jet is an efficient mixing mechanism ensuring fast equalising of the jet temperature and the environment.

It follows from literature data and performed experiments that the cone angle of a cryogenic jet can be considered as constant, of about 13 degrees. It does not depend either on the orifice diameter or on the gas vented.

The average velocity in any cross section of a jet which is further than 0.2 m from the jet orifice can be calculated from a simple model based on momentum conservation.

Heat transfer between jet and any solid object which is further than 0.2 m from the jet orifice can be calculated using a dimensionless equation (16).

5. Acknowledgements

The authors would like to thank Philippe Lebrun, Laurant Tavian and Wolfgang Erdt for helpful suggestions and support of the study, Norbert Franielczyk and Tomasz Zuk from BOC Gazy and Helex for the help in experiments.

6. References

[1] M. Chorowski, B. Hilbert, L. Serio, L. Tavian, U. Wagner, R. van Weelderen, Helium recovery in the LHC cryogenic system following magnet resistive transitions, Advances in Cryogenic Engineering, Vol. 43. p. 467 - 474

[2] M. Chorowski, B. Skoczen, Thermo-mechanical analysis of cold helium injection into gas storage tanks made of carbon steel following resistive transitions of LHC magnets, Proc. of the Seventeenth International Cryogenic Engineering Conference, Institute of Physics Publishing, Bristol and Philadelphia, 1998, p. 755 – 758

[3] M. Chorowski, B. Skoczen, Thermo-mechanical analysis of cold helium injection into medium-pressure (MP) gas storage tanks following resistive transition of a LHC sector, LHC Project Note 119, 1997

[4] J. Madejski, Wymiana ciepla (Heat exchange, in Polish), PWN, Warszawa, 1978